Purdue University
Purdue e-Pubs

International Compressor Engineering Conference | School of Mechanical Engineering

2008

Suction Pulsations and Flow-Induced Noise in Reciprocating Compressors

Christian Svendsen
Danfoss Compressors GmbH

Jens Erik Nissen
Danfoss Compressors GmbH

Sven Eric Nielsen
Danfoss Compressors GmbH

Preben Bjerre
Danfoss Compressors GmbH

Suction Pulsations and Flow-induced Noise in Reciprocating Compressors

Christian Svendsen*, Jens Erik Nissen, Sven Eric Nielsen, Preben Bjerre

Danfoss Compressors GmbH
Mads-Clausen-Strasse 7, D-24939 Flensburg, Germany
Phone: +49 461 4941 236; Fax: +49 461 4941 629; E-mail: c.svendsen@danfoss.de

ABSTRACT

This investigation demonstrates that the upstream flow relative to the suction valve can have a significant influence on the noise emitted during the suction process. Specifically, a noise problem on a customer appliance was detected in the 1 kHz 1/3-octave band. The excitation mechanism of the appliance was caused by suction pulsations. The compressor shell itself did not radiate any notable noise in that band, which is mainly due to the fact, that the muffler has a direct suction admission via a flexible telescope. The unexpected noise source appeared when changing the design of the muffler outlet tube, which connects the muffler volume with the suction port. The noise phenomenon is investigated theoretically and experimentally, and a new muffler design with improved acoustical properties is proposed.

1. INTRODUCTION

The suction noise emitted by the UFO-compressors has been minimized by introducing a direct suction admission via a completely tight telescope. The modification of the suction noise transmission path can, however, result in higher pulsation levels at certain frequencies. The increase of the pulsation level can to some extent be compensated for by an increase in the muffler volume. In the original design, the muffler outlet tube had a smooth 90^0 bend towards the suction port. In order to obtain a smooth bend, the outlet tube had to be assembled from three plastic parts, which also complicated the assembling of the cylinder cover and valve system. In the following, this design is referred to as Design A. In an effort to reduce the production cost and increase the production capacity, a new outlet tube was designed. The new outlet tube was integrated into the upper part of the muffler and, therefore, a single injection moulding tool could be used. With this modification a sharp edge close to the suction port had to be introduced. This design is referred to as Design B. Subsequent suction pulsation measurements up to the 10^{th} harmonic showed nothing out of the ordinary. Some time after the introduction, however, a noise problem in the 1 kHz 1/3-octave band of a customer appliance was observed. The noise problem was caused by suction pulsations around the 20^{th} harmonic, which is far above the 10^{th} harmonic of the ordinary pulsation measurements. The pulsation problem was solved by introducing changes to the interior design of muffler, which did not involve the outlet tube. This final design is referred to as Design C. A large amount analysis work has been performed in the process of reducing the suction pulsation level. In this article some of results of the analysis work will be presented.

The article is organized as follows: In Section 2 the muffler designs are described in detail and in Section 3 the noise measurements on the customer appliance with the three designs are presented. Section 4 summarizes some of the numerical and experimental analysis work performed on suction pulsations. Finally, in Section 5 aeroacoustic measurements of flow-induced noise radiated from the two muffler outlet tube variants are presented.

2. INVESTIGATED MUFFLER DESIGNS

In this section the investigated muffler designs are described in detail. Figure 1 shows cross-sectional views of the three muffler designs. The first three leftmost views show an assembly of the muffler and the cylinder cover from the side. The valve plate and the cylinder, which are not displayed, are positioned to the left of these views. The muffler cavity is obtained by welding a lower (gray) and an upper (green) plastic part together. Within the muffler cavity, Design A and B have a flow guidance tube (gray), which directs the flow up and towards the muffler outlet tube (green). The guidance tube of Design C, which is indicated by a brown color, points into the middle of the muffler cavity. The direction of the guidance tubes can also be seen in the right-hand side of Figure 1, which shows a cross-sectional view from the back of the muffler cavity. The exit flow direction of the guidance tube is indicated by black arrows. The direction of the guidance tube of Design C has solely been dictated by acoustic considerations;

this will be explained in detail in Section 4. Flow directions at the inlet and outlet portions of the muffler are indicated by black arrows in the leftmost view of Design A. Furthermore, a flow separation point of Design B and C, which is considered to be important in this study, is pointed out by red arrows.

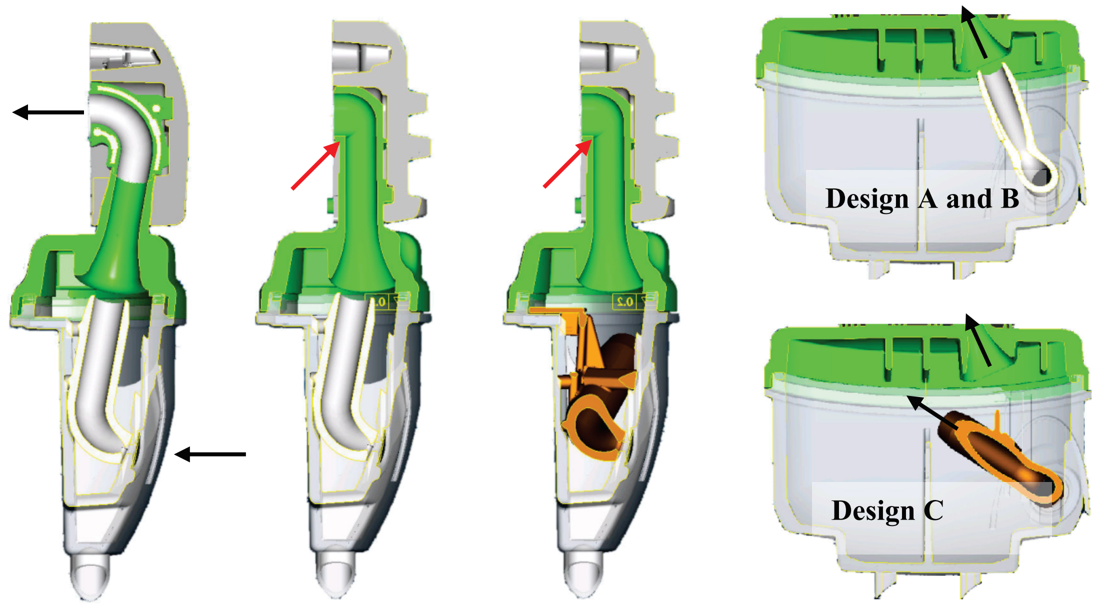

Design A **Design B** **Design C**

Figure 1: Overview of muffler designs: Black and red arrows indicate the flow directions and the flow separation point, respectively.

Figure 2 shows the result of a steady CFD simulation which illustrates the presence of the flow separation point and its effects further downstream e.g. the presence of recirculation zones etc. The muffler outlet tube is situated to the right, where the flow is forced to make a left turn; thereafter it passes the valve and enters the cylinder cavity. The flow velocity magnitude plot of Design B and C shows, that a significant flow separation point is present in the outlet tube. The flow separation point is indicated by a red arrow in Figure 2. In an unsteady flow the separation point would be the source of eddies, which are shed into the flow towards the suction port.

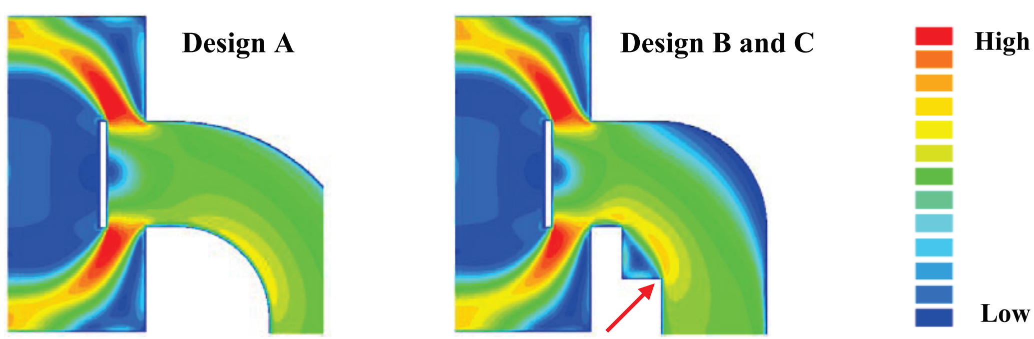

Figure 2: Flow velocity magnitude plot illustrating the downstream effect of the separation point, which is indicates by a red arrow.

In the following sections, it will be shown that the designs behave very differently with respect to suction pulsations at higher frequencies.

3. APPLIANCE EXCITATION BY SUCTION PULSATIONS

Figure 3 shows the sound power measurements of a customer appliance, which was fitted with an NLX8.8KK2 compressor. A marked increase in the 1 kHz band and the neighboring bands is observed when replacing Design A with Design B, see Figure 3.

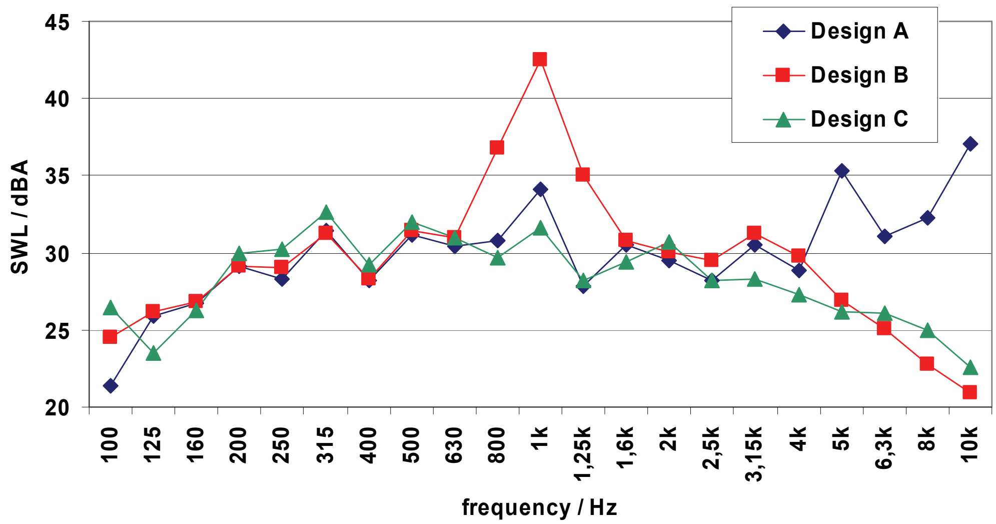

Figure 3: Measured sound power level of appliance with NLX8.8KK2 compressor.

Since the compressor is fitted with a tight telescope between the compressor inlet connector and muffler inlet, no significant noise radiation from the compressor shell around 1 kHz could be detected. Furthermore, Design A and B are acoustically nearly identical; the only difference is that the acoustic length of the outlet tube is L = 52 mm and L = 48 mm for Design A and B, respectively. The preliminary conclusions were that the excitation of the appliance was caused by suction pulsations and that the source strength had increased from Design A to B. The proposed Design C has the same source strength as Design B, but it has been altered acoustically in order to lower the suction pulsations around 1 kHz, see the last trace in Figure 3. The above conclusions are further quantified in the next section.

4. CALCULATED AND MEASURED SUCTION PULSATIONS

In order to clarify the acoustic phenomena at hand some numerical acoustics calculations have been performed and the results of these calculations are then compared with experimental suction pulsation data.

4.1 Acoustic boundary element calculations

Boundary element models of all three muffler designs have been constructed and the direct boundary element method has been used to solve the acoustics. In order to reduce the calculation effort, each model has been split into five internal domains, which are coupled by velocity and pressure boundary conditions at their interfaces. The largest zone, which primarily determines the calculation effort, has less than 2000 elements. At the end of the muffler flow outlet tube, which is next to the suction port, a frequency independent unit velocity boundary condition has been applied. At the flow inlet hole of the muffler a long termination tube, which is more than 12 diameters long, has been placed. This should ensure that a nearly anechoic termination is obtained when applying free field acoustic impedance at the end of the tube. Furthermore, the muffler boundaries have infinite impedance i.e. no additional damping besides the anechoic termination is present. For the time being it is assumed that these boundary conditions resemble those of the suction pulsation measurements. Figure 4 shows the sound pressure level inside the termination tube of Design B and C. The sound pressure level of Design A has not been shown because it is nearly identical to that of Design B.

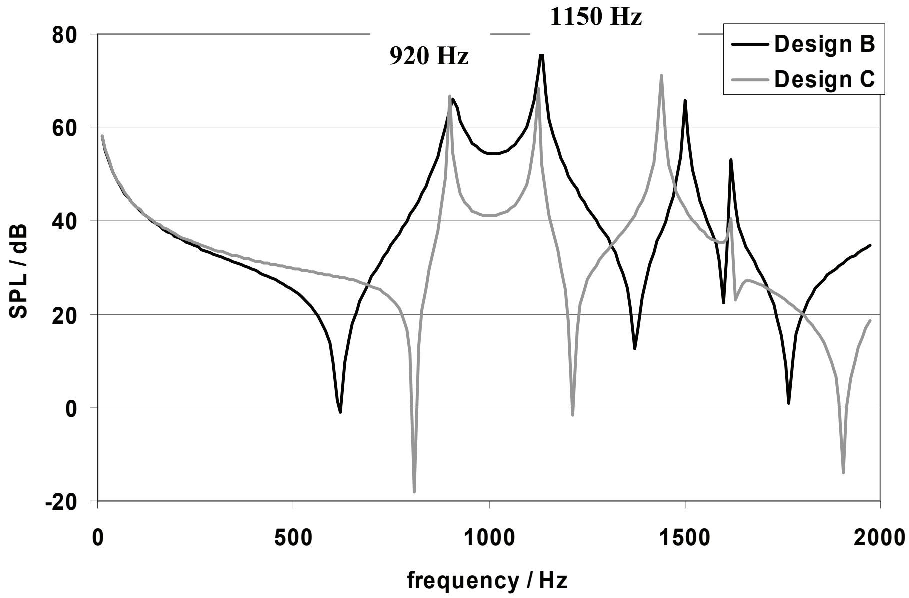

Figure 4: Calculated pulsation level in an anechoic flow inlet tube of the muffler.

For both designs, local sound pressure maxima are observed at 920 and 1150 Hz. Notice that the sound pressure of Design C around 1 kHz is more than 15 dB lower than that of Design B. This explains why Design C in the appliance performs reasonably well around 1 kHz relative to Design B, see Figure 3. The internal sound pressure distribution of the local pressure maxima are displayed in Figure 5. It is seen, that the first peak at 920 Hz is due to an acoustic resonance in the muffler cavity with a pressure gradient predominantly in the horizontal direction. The second acoustic resonance at 1150 Hz points in the horizontal and vertical direction within the left and right section of the muffler, respectively.

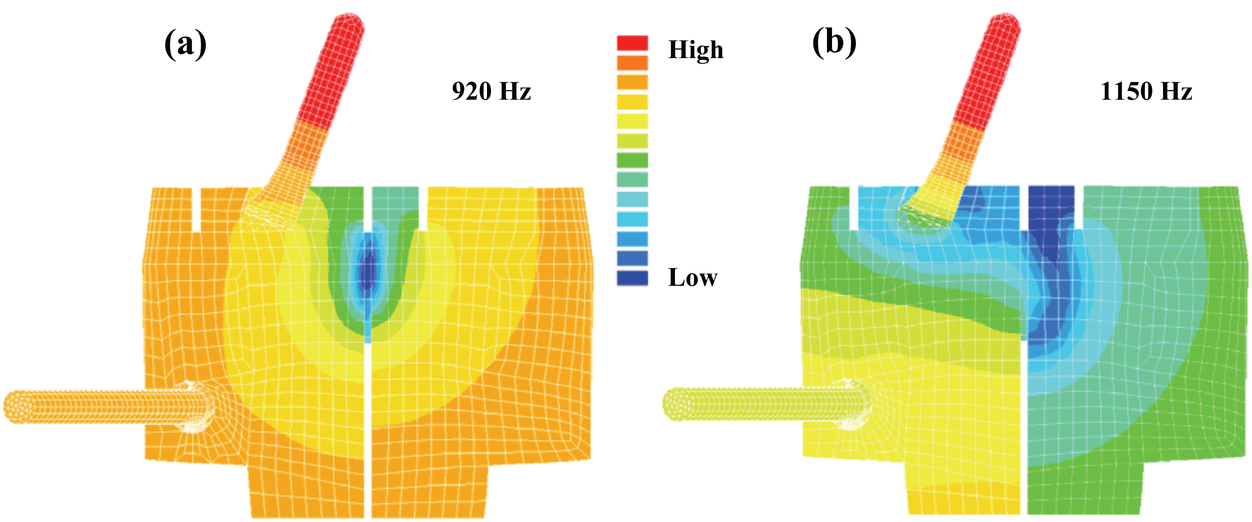

Figure 5: Front view of the suction muffler: Internal sound pressure distributions on the muffler walls of the two acoustic resonances at (a) 920 Hz and (b) 1150 Hz.

In Figure 1 it is seen, that the major difference between Design B and C is the direction of the flow guidance tube. In Design C the open end of the tube has been positioned so that it is close to the spatial pressure minima of the two acoustic resonances. In this way, the transmission of suction pulsations to the appliance can be minimized. The solution strategy is similar to that reported by Suh *et al*. (2000). In the following section, the thus obtained sound pressures will be compared with the measured suction pulsation levels.

4.2 Comparison between measured and calculated pulsation level differences

The suction pulsation level has been measured by use of a PCB-116B piezoelectric pressure transducer connected to a Brüel & Kjær PULSE analyzer. FFT spectra of the suction pulsations were measured up to the 30th harmonic with 1 Hz resolution. The observed harmonics were very narrow with a band width from peak to back ground level of less than 5 Hz. The total pulsation level of each harmonic was integrated within that band width. The NLX8.8KK2 compressor was operated with R600a at suction and discharge pressures equivalent to -25^{0}C evaporation and 55^{0}C condensation temperatures, respectively.

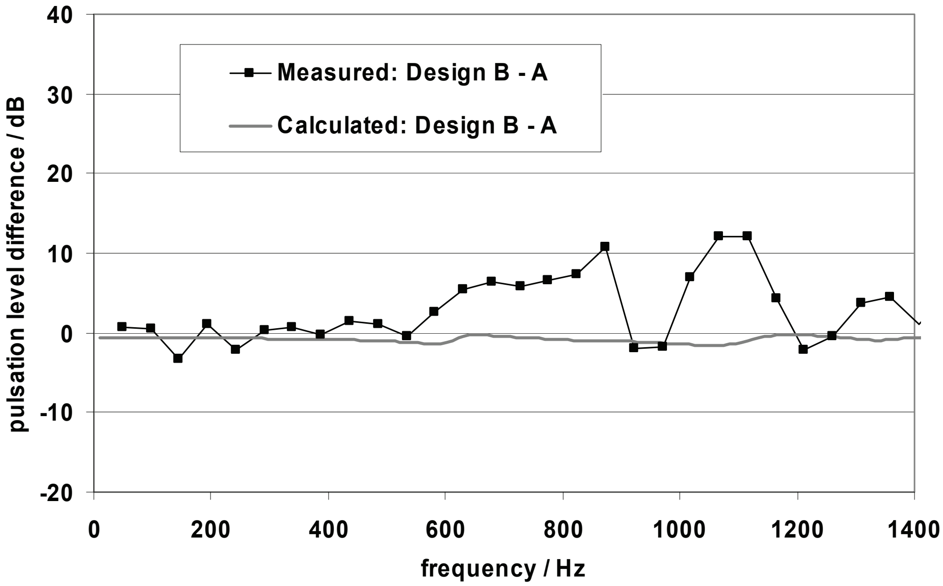

Figure 6: Comparison between measured and calculated pulsation level difference between Design B and A.

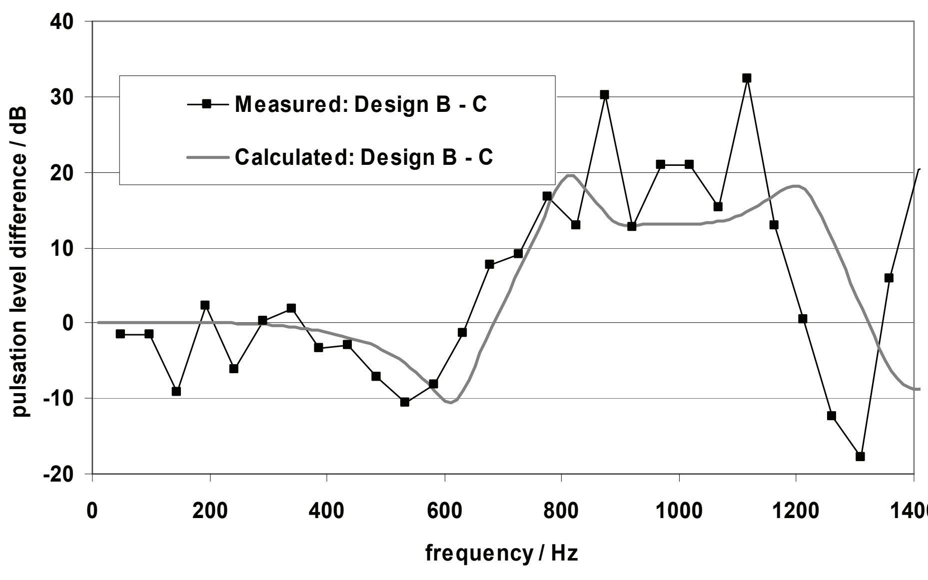

Figure 7: Comparison between measured and calculated pulsation level difference between Design B and C.

The pressure transducer is flush mounted within a brass casing, which is an integrated part of the gas supply line. In the upstream direction, the gas supply line consists of the following elements: Compressor suction connector, 1 m flexible hose, transducer casing, 0.7 m flexible hose and, finally, a 10 m curled cobber tube. From the compressor suction connector and upstream the tube diameter is 8.0 mm. The suction supply line cannot have a perfectly anechoic termination due to the multiple surface impedance changes along tubing and the abrupt termination of the curled copper tube (Lai and Soedel, 1996). However, by calculating the pulsation level difference between two designs the interference effects of the termination can be nearly cancelled out.

A direct comparison between the calculated and measured suction pulsation pressures cannot be performed since in this work the source strength and source impedance is unknown. Measurements of the source characteristics of the suction port has been performed by Ih *et al* .(1998). The dependence on the source strength can be removed by calculating the pulsation level difference between two designs. The source impedance, however, cannot be removed by this operation. Figure 6 shows the pulsation level difference between Design B and A. The calculated level difference indicates that the acoustic properties of the two designs are nearly equal. However, a significant difference between the measured suction pulsation levels can be seen. This suggests that the source strength has increased considerably when introducing Design B.

The level difference between Design B and C is displayed in Figure 7. In this case, a better correspondence between the measured and calculated level difference is observed. At some frequencies, however, the deviations are of the same order of magnitude as those seen in Figure 6. The good correspondence indicates, that the difference between these two designs is entirely determined by the acoustic properties of the muffler and that the sources are nearly identical. Finally, it should be noted that unlike the calculations shown in Figure 4, a finite and real valued impedance equaling 100·ρc of the muffler boundaries has been used. This is done in order to introduce damping effects into the calculation. These damping effects have been observed experimentally (Svendsen, 2004). The mechanism of the increased source strength, which is seen in Figure 6, cannot be found by use the above acoustic calculations. In the next section, aeroacoustic measurements on the outlet tube show that a difference in the source strength can be observed.

5. AEROACOUSTIC MEASUREMENTS ON OUTLET TUBES

Figure 8(a) shows schematically the experimental set-up, which is used to measure the flow-induced noise of the muffler outlet designs. The set-up is operated with air and it is situated inside a reverberation chamber in which the emitted sound power can be measured.

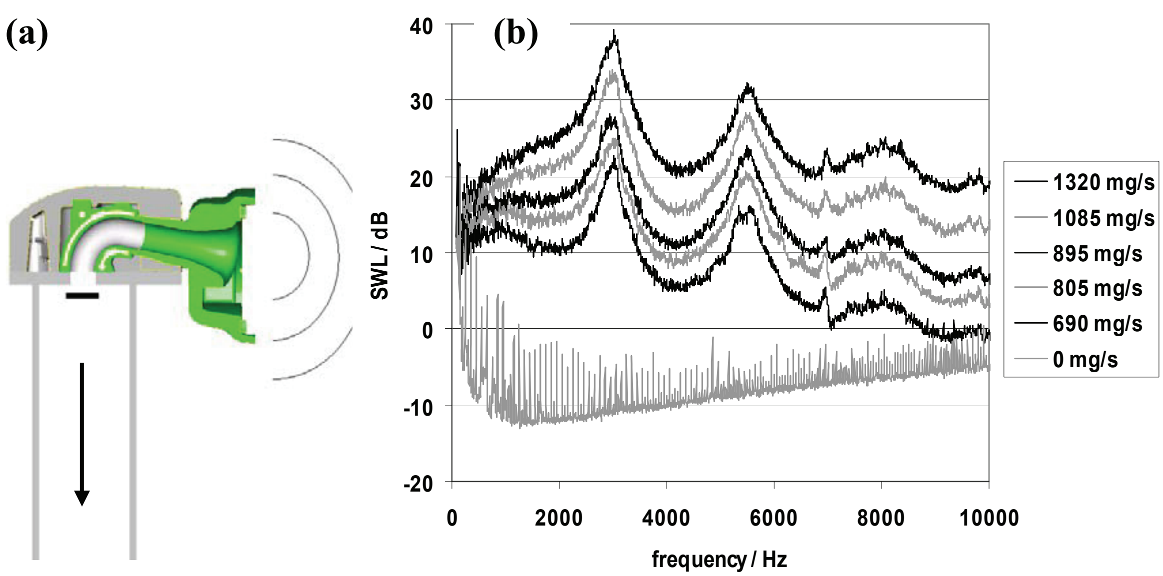

Figure 8: (a) Experimental set-up from which flow-induced noise is radiated. (b) Measured sound power of Design A at various mass flow rates.

The flow is generated by a lower pressure on the cylinder side. The lower pressure is obtained by use of a 25 m long hose, which is connected to an evacuation line outside the chamber. In figure 8(a) the flow direction inside the first part of the hose is indicated by a black arrow. The horizontal bar below the suction hole indicates the suction valve, which is completely immobilized, and the average distance over the valve seat is 2.6 mm. The arrangement only measures the noise emitted from the outlet tube, while that transmitted down the hose will escape the measurement. Noise from the evacuation line above the back ground level could not be detected when operating the set-up with the hose alone. The mass flow rate was measured by use of a flow meter (MASSFLO MASS 2100), which was inserted between the hose and the evacuation line. The uncertainty of the measured mass flow rate is estimated be 10-20 mg/s. Figure 8(b) shows the measured sound power level spectrum of Design A at various mass flow rates. The sound power level has been obtained by use of a reference source (Brüel & Kjær Type 4204). Here it should be noted, that the reported sound power spectra have been obtained by use of a FFT analyzer with 4 Hz resolution rather by a CPB analyzer with 1/3-octave band resolution. The calibration levels, however, are only given with 1/3-octave band resolution and therefore an interpolation procedure had to be employed in order to obtain the sound power levels with 4 Hz resolution. It is seen that the curves do not cross and that the level increases with increasing mass flow rate. A similar behavior of Design B was observed.

Clearly some sort relationship between the radiated sound power and the mass flow rate must exist. This can in some special cases be gives in terms of a power-law relationship. A good introduction to this subject is given by Barenblatt (2003) and the references cited therein. To simply the problem, it is assumed that the phenomenon depends on only six quantities: (1) a flow length scale l, (2) a flow velocity scale v, (3) the density ρ, (4) the speed of sound c, (5) an acoustic length L and (6) a frequency f. Here l could be the valve lift and v the average velocity through the valve opening. In this case, v would be in proportion to the mass flow rate. Furthermore, L is here the length of the outlet tube, which is L = 52 mm and L = 48 mm for Design A and B, respectively.

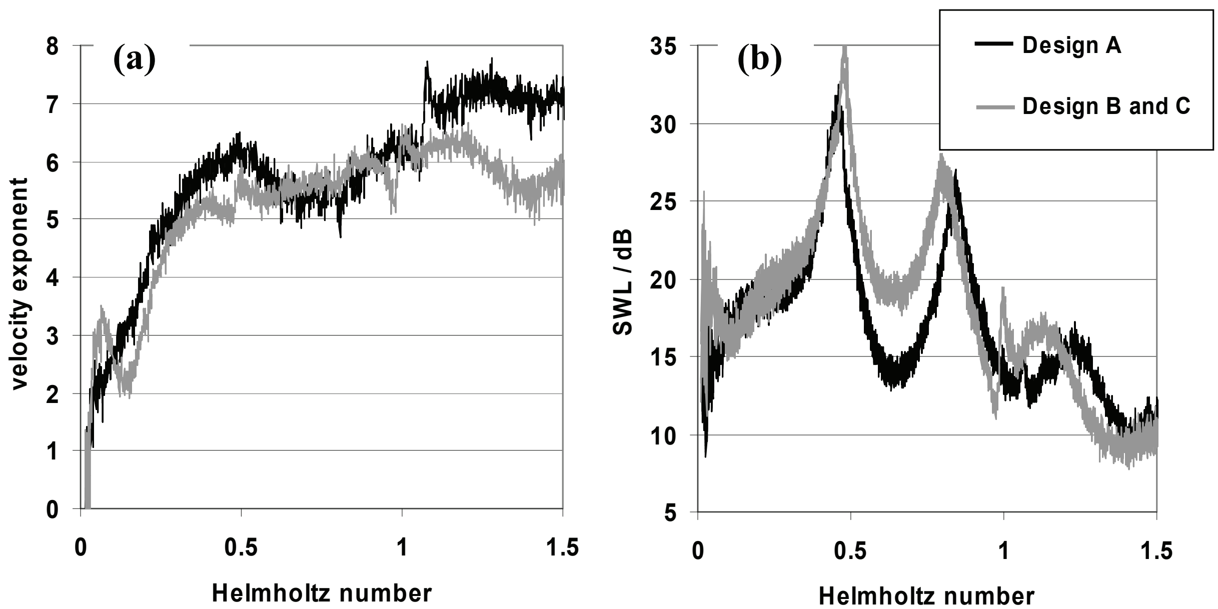

Figure 9: (a) The calculated velocity exponent versus Helmholtz number. (b) All measured sound power curves, which are rescaled to the same mass flow rate (=1000 mg/s).

It is seen that the above mentioned quantities are not dimensionally independent. In this case, there are three independent quantities and three dependent ones. The latter can be written as a power-law monomial of the independent quantities. We can for instance use l, v and ρ as the independent quantities and from these and the remaining quantities construct three dimensionless ones. In aeroacoustics, the obvious choice for the dimensionless quantities would be the Mach number, $Ma = v/c$, the Helmholtz number, $He = fL/c$ and the Strouhal number, $St = fl/v$. According to the Π-theorem (Barenblatt, 2003), the radiated sound power can be written as follows:

$$SW = \rho\, v^3\, l^2\, \Phi(Ma,He,St), \tag{1}$$

where Φ is some dimensionless function. Some hints to the form of this function can be found by inspecting the Flowcs Williams-Hawkings equation (Dowling and Ffowcs Williams, 1983; Howe, 1998), which is a generalisation of Lighthill's acoustic analogy applied to a finite volume in the presence surfaces. Some trial and error on the measurement data revealed, that the data can be described by the following power-law relationship:

$$SW = \rho\, v^3\, l^2\, \Phi(He)\, Ma^{n(He)}, \qquad (2)$$

where $n(He)$ is a Helmholtz number dependent exponent of Mach number. Since the Mach number is in proportion to the velocity (and mass flow rate), the sound power will be in proportion to the velocity (and the mass flow rate) to the power of $3+n(He)$. This quantity is referred to as the velocity exponent. The velocity exponent can for instance be found by taking the logarithm of Eq.(2) and use linear regression to find the slope, $3+n(He)$, for each Helmholtz number. Figure 9(a) shows the thus obtained velocity exponent versus the Helmholtz number. It is seen that for $He > 0.5$, the sound power increases to around the sixth power of the velocity. This indicates that it is primarily dipole noise, which is radiated from the surface (Dowling and Fflowcs Williams, 1983). By use of Eq.(2), the SWL curves, can for instance be rescaled to the same mass flow rate (=1000 mg/s). The collapse of the curves confirms the power-law relationship. Note, that in the interval $He = 0.4 – 0.8$, the sound power radiated from Design A is significantly lower than that radiated from Design B, and that the acoustic resonances of the tubes can be clearly distinguished. Ideally, the resonances would the close to $He = 0.5, 1.0, 1.5$ etc. However, since no end corrections are added to the acoustic lengths, the resonances will appear at lower Helmholtz numbers.

7. CONCLUSIONS

In this case study the following has been demonstrated:

- That the source strength of the suction process can be changed significantly when changing the design of the muffler outlet tube.
- Aeroacoustic measurements have been performed with a steady air flow at various mass flow rates through the muffler outlet tube. They indicate that dipole sources are dominant at $He > 0.4$ and that an outlet tube with sharp edges radiates more noise in the interval $He = 0.4 – 0.8$.
- The suction pulsation level of the muffler design can be significantly reduced by changing the acoustic properties of the muffler.

NOMENCLATURE

L	acoustic length	(m)	SW	sound power	(Watt)
l	flow length	(m)	SWL	sound power level	(–)
f	frequency	(s^{-1})	He	Helmholtz number	(–)
v	flow velocity	(m/s)	Ma	Mach number	(–)
c	speed of sound	(m/s)	St	Strouhal number	(–)
ρ	density	(kg/m^3)			

REFERENCES

Barenblatt, G.I., 2003, *Scaling*, Cambridge University Press, United Kingdom, p. 171.

Dowling, A.P., Ffowcs Williams, J.E., 1983, Sources of sound, *In: Sound and sources of sound*, Ellis Horwood Limited, England: p. 146-167.

Howe, M.S., 1998, Aerodynamic sound in unbounded flows, *In: Acoustics of fluid-structure interactions*, Cambridge University Press, United Kingdom: p. 101-156.

Ih, J.-G., Jang, S.-H., Kim, S.-J., Shim, J.-S., 1998, Measurements of the acoustic source characteristics of the intake port in the refrigerator compressor, *Proc. of the 14th Intenational Compressor Engineering Conference at Purdue*: p. 561-564.

Lai, P. C.-C., Soedel, W., 1996, On the anechoic termination assumption when modelling exit pipes, *Proc. of the 13th Intenational Compressor Engineering Conference at Purdue*: p. 815-820.

Suh, K.-H., Kim, J.-D., Lee, B.-C., Kim, Y.-H., 2000, The analysis on the discharge muffler in the rotary compressors, *Proc. of the 15th Intenational Compressor Engineering Conference at Purdue*: p. 651-656.

Svendsen, C., 2004, Acoustics of suction mufflers in reciprocating hermetic compressors, *Proc. of the 17th Intenational Compressor Engineering Conference at Purdue*: C029.